A temporal thymic selection switch and ligand binding kinetics constrain neonatal Foxp3+ T_reg cell development

Brian D. Stadinski[1,3], **Sydney J. Blevins**[1,3], **Nicholas A. Spidale**[1], **Brian R. Duke**[1], **Priya G. Huseby**[1], **Lawrence J. Stern**[1,2], **Eric S. Huseby**[1,*]

[1]Department of Pathology, University of Massachusetts Medical School Worcester, MA 01605, USA.

[2]Department of Biochemistry & Molecular Pharmacology, University of Massachusetts Medical School Worcester, MA 01605, USA.

[3]These authors contributed equally to this work

Abstract

The neonatal thymus generates Foxp3+ regulatory T (tT_reg) cells that are critical in controlling immune homeostasis and preventing multi-organ autoimmunity. The role of antigen specificity on neonatal tT_reg cell selection is unresolved. Here we identify seventeen self-peptides recognized by neonatal tT_reg cells, and reveal ligand specificity patterns that include self-antigens presented in an age-dependent and inflammation-dependent manner. Fate mapping studies of neonatal Peptidyl arginine deiminase, type IV, (Padi4)-specific thymocytes reveal disparate fate choices. Neonatal thymocytes expressing TCRs that engage IA^b-Padi4 with moderate dwell times within a conventional docking orientation are exported as tT_reg cells. In contrast, Padi4-specific TCRs with short dwell time are expressed on CD4+ T cells, while long dwell times induce negative selection. Temporally, Padi4-specific thymocytes are subject to a developmental stage-specific change in negative selection, which precludes tT_reg cell development. Thus, a temporal switch in negative selection and ligand binding kinetics constrains the neonatal tT_reg selection window.

Introduction

αβ T cell development creates a repertoire of immature thymocytes expressing T cell receptors (TCRs) with a graded scale of reactivity for self-peptides presented by host-Major Histocompatibility Complex molecules (self-pMHC). The fate of these immature thymocytes is then guided by TCR signals emanating from the engagement of self-pMHC ligands. It has been well established that weak TCR signals are required for positive selection, thereby ensuring mature T cells are capable of recognizing MHC displayed ligands, while strong TCR signals often result in the clonal elimination of thymocytes, limiting the risk of autoimmunity[1, 2]. Despite these highly ordered molecular and cellular processes, some overtly self-reactive and tissue-specific antigen (TSA)-reactive T cells are exported from the thymus and are maintained within the mature conventional T (T_{conv}) cell repertoire. Limiting the autoimmune potential of self-reactive T_{conv} cells are several additional T cell lineages, including thymus-derived T regulatory cells that express the transcription factor Foxp3 (tT_{reg} cells).

The neonatal exposure of thymocytes to self-antigens and the development of tT_{reg} cells are critical for enforcing immune tolerance and preventing autoimmunity. Depletion of tT_{reg} cells in mice, as well as mouse models that limit self-antigen display by mTECs results in multi-organ autoimmunity[3–7]. Further, tT_{reg} complementation studies in NOD mice suggest that adult-derived tT_{reg} cells are unable to fully limit autoimmunity when tT_{reg} cells generated in the first 10 days of life are absent. This phenomenon correlated with the observation that distinct tT_{reg} clonotypes are selected in the perinatal and neonatal thymus as compared to the adult thymus[4].

How recognition of self-ligands by neonatal thymocytes influence lineage fate decisions remains incompletely understood. Following positive selection, thymocytes expressing MHC-II restricted TCRs upregulate TCR and chemokine receptor 7 (CCR7) expression, migrate to the medulla and differentiate into semi-mature and then mature CD4^{+} single positive (CD4SP) cells, eventually to be exported from the thymus[8–10]. During the CD4SP stage, thymocytes that engage self-pMHC presented by medullary epithelial cells (mTECs) or thymic dendritic cells (DC) can be diverted into the tT_{reg} lineage, undergo a second wave of deletion, or continue along the CD4 T_{conv} cell differentiation process[2, 9, 11–14]. Self-tolerance and the development of a subset of tT_{reg} cells generated in the first week of life requires *Aire*-dependent presentation of self-ligands[4, 15], though the specific *Aire*-dependent and *Aire*-independent self-epitopes that regulate neonatal thymic development are largely unknown. Observations that perinate- and adult-derived tT_{reg} cells express differing TCR clonotypes have suggested a role for age in the selection of particular antigen-specificities[4]. However, the dearth of identified tT_{reg} self-ligands[16–21], and minimal ability to monitor neonatal and adult thymic selection of antigen-specific tT_{reg} cells within polyclonal repertoires has limited the ability to define the molecular basis for tT_{reg} selection.

Here we investigated the TCR:self-pMHC ligand recognition properties that regulate the neonatal window of T cell development. We observed that TCRs expressed on neonatal tT_{reg} cells can recognize self-antigens whose presentation on antigen-presenting cells (APCs) is regulated by age and inflammation. A self-antigen discovery platform was created, and used

to identify a panel of ligands recognized by neonate-derived tT_{reg} cells, including Peptidyl arginine deiminase, type IV (Padi4). The development of Padi4-specific T cells is restricted to the neonatal thymus; alterations in the adult thymus lead to Padi4-specific thymocytes undergoing negative selection at the $CD4^+CD8^+$ (DP) $CCR7^{neg}$ to $CCR7^{pos}$ transition, thereby eliminating the precursor cells of Padi4-specific tT_{reg} cells and $CD4^+$ T_{conv} cells. Within the neonatal thymus, the CD4SP selection branch point correlated with TCR:pMHC dwell time of binding. Specifically, moderate $TCR:IA^b$-Padi4 dwell times instruct neonatal tT_{reg} cell development, whereas longer dwell times induce negative selection, and short dwell time TCRs are expressed on mature $CD4^+$ T_{conv} cells. Our results provide insight into the ligand specificity of the neonatal tT_{reg} repertoire, and reveal roles for age-dependent alterations in negative selection and TCR:pMHC binding kinetics in framing the neonatal T cell selection window.

RESULTS

Neonatal tT_{reg} TCRs can recognize steady state and inflammation-dependent antigens—To test levels of self-reactivity carried within the neonatal tT_{reg} repertoire, we cloned 66 TCRs expressed on Foxp3-GFP$^+$ CD25$^+$ CD4$^+$ thymocytes isolated from 2-week old $Tcra^{+/-}$ C57BL/6, and 316 TCRs from 2-week old $Tcra^{+/-}$Yae62β Tg mice (transgenic mice that express a fully rearranged TCRβ chain). $Tcra^{+/-}$ mice were used to ensure that the thymocytes expressed only a single TCRα chain paired with the expressed TCRβ chain. Cloned TCRs were re-expressed in a TCR-deficient hybridoma, 5KC TCRαβ^{null} that also expresses mouse CD4, and tested *in vitro* for responses to syngeneic APCs. Analyses of C57BL/6-derived tT_{reg} hybridomas revealed three self-reactivity categories: 14% were reactive to resting adult splenic APC, 9% either required, or were >3-fold more reactive to adult splenic APCs isolated from mice pretreated with lipopolysaccharide (LPS) plus anti-CD40 (LPS+αCD40) to induce inflammation, and 77% have self-reactivity that is below the detection of this assay (Fig. 1a,b). Yae62β$^+$ tT_{reg} hybridomas demonstrated an ~1.5-fold increase in frequencies of these self-reactivity categories (Fig. 1c,d).

Neonatal tT_{reg} hybridomas were found to differentially recognize specific APC subsets. The B6–50.1 C10 and 6287 tT_{reg} hybridomas recognize antigens similarly presented on resting and LPS+αCD40 activated DC populations (Fig. 1e,f), while the B6–13 and 4699 tT_{reg} hybridomas showed increased reactivity to LPS+αCD40 activated DCs (Fig. 1g,h). Additional tT_{reg} hybridomas were found to specifically recognize B cell presented antigens (Supplementary Fig. 1). ~70% of the *in vitro* self-reactive neonatal tT_{reg} hybridomas are more reactive to adult as compared to neonatal splenocytes (Fig. 1i,j). The characterization of neonatal tT_{reg} TCRs derived from Yae62β Tg mice allowed for TCRα sequencing methods to associate clonotype frequencies with self-reactivity properties. High throughput sequencing of Vα2$^+$ tT_{reg} cells, isolated from neonatal and adult YAe62β mice, revealed that tT_{reg} cells with specificity for age-dependent antigens are selectively enriched in the neonatal thymus as compared to the adult thymus (Fig. 1k). Collectively, these data are consistent with the requirement for specific DC subsets in the thymic selection and peripheral activation of certain tT_{reg} clonotypes *in vivo*[14, 22], and support the hypothesis that neonatal tT_{reg} cells can recognize age- and inflammation-dependent changes in antigen presentation.

Identification of self-pMHC epitopes recognized by neonatal tT$_{reg}$ cells TCRs

—To characterize potential self-peptides recognized by neonatal tT$_{reg}$ cells, we curated mass spectrometry approaches that assessed the IA^b immunopeptidome and synthesized the unique species to create an IA^b self-peptide library (see Methods). Eighty individual neonatal tT$_{reg}$ hybridomas were cultured with pools of self-peptides and IA^b expressing fibroblasts as the APC, and IL-2 secretion was measured. T cell specificity for an individual peptide was de-convoluted from the reactivity patterns. Using this method, seventeen unique self-peptides were identified that stimulated at least one neonatal tT$_{reg}$ hybridoma with an EC$_{50}$ value of 1μM or less (Fig. 2a, Supplementary Table 1).

The 4699 tT$_{reg}$ hybridoma was found react to Peptidyl arginine deiminase, type IV, (Padi4$_{92-105}$), and the 6287 T cell hybridoma recognizes Adducin 2 (Add2$_{606-621}$) (Fig. 2b,c). Activation assays using splenocytes from *Padi4$^{-/-}$* mice and *Add2$^{-/-}$* mice demonstrated that the *in vitro* self-reactivity of the 4699 and 6287 tT$_{reg}$ hybridomas required their identified self-ligand (Fig. 2d,e). IA^b tetramers carrying Padi4$_{92-105}$ and Add2$_{606-621}$ were created, and found to specifically stain the 4699 and 6287 tT$_{reg}$ hybridomas, respectively (Fig. 2f,g). The ability of these self-pMHC tetramers to stain tT$_{reg}$ hybridomas suggested that these reagents would allow for visualization of the Padi4-and Add2- specific tT$_{reg}$ repertoires *in vivo*.

Development of Padi4-specific tT$_{reg}$ cells is restricted to the neonatal period—

Padi4- and Add2-specific Vα2$^+$ CD4SP thymocytes are readily detected using self-pMHC tetramers in one to three week old YAe62β mice, with many further differentiating into tT$_{reg}$ cells. These Foxp3-GFP$^+$ tT$_{reg}$ express the classical phenotypic markers including CD25, GITR, PD-1 and CD44 (Fig. 3a, top row, Supplementary Fig. 2a). Starting at 4wks of age, a severe depletion of both Padi4-reactive thymic CD4SP and tT$_{reg}$ cells was observed, (Fig. 3a, bottom row). Analyses of *Padi4$^{-/-}$* mice revealed that the neonatal development of Padi4-specific tT$_{reg}$ cells, and the adult loss of Padi4-specific CD4SP are dependent upon the expression of the identified self-antigen (Fig. 3b). The age-dependent alteration of the Padi4-specific thymocyte repertoire occurs both as a percent of total cells, and as an absolute number of cells (Fig. 3c–f). Thus, development of Padi4-specific tT$_{reg}$ stops in the adult thymus, and is not simply diluted out by changes in thymic cellularity. A similar age-dependent tT$_{reg}$ selection occurs for Add2-reactive thymocytes (Supplementary Fig. 2b–d). Further, the high frequencies of IA^b-Padi4 tetramer bright CD4SP thymocytes in 6 weeks old *Padi4$^{-/-}$* YAe62β indicate thymocytes can rearrange Padi4-specific TCRs in adult mice (Fig. 3b). These data demonstrate that the development of Padi4-specific tT$_{reg}$ cells is unique to neonatal thymus.

Within the mature T cell repertoire accumulation of Padi4-reactive tT$_{reg}$ cells in the spleen begins at 1 week of age, and requires expression of endogenous Padi4 (Fig. 4a–f). As a percentage of the total, Padi4-reactive tT$_{reg}$ cells are diluted correlating with the age-dependent reduction in thymic output (Fig. 4c). The total number Padi4-reactive tT$_{reg}$ cells within the spleen peaks at four weeks, and slowly decrease through 8 weeks of age (Fig. 4d). An early accumulation of Padi4-specific CD4$^+$ T$_{conv}$ cells similarly develops (Fig. 4e, f). Splenic Padi4-reactive tT$_{reg}$ cells share phenotypic similarity with perinatal tagged tT$_{reg}$ subsets[4], including high expression levels of PD-1, CD44, CD25, GITR, NRP1 and CTLA4

(Fig. 4g). The corresponding $CD4^+$ T_{conv} cells in these mice express PD-1, NRP1, CD73 and FR4 (Supplementary Fig. 3), a phenotype similar to studies of antigen-experienced anergic CD4 T cells[23]. In contrast, Padi4-reactive T cells that developed in $Padi4^{-/-}$ mice are almost exclusively $CD44^{lo}CD62L^{hi}$ naïve-phenotype CD4 T_{conv} cells (Supplementary Fig. 3).

The increased reactivity of the 4699 tT_{reg} hybridoma to LPS+αCD40-activated APCs (Fig. 1f) suggested that Padi4-specific tT_{reg} cells might sense inflammation *in vivo*. To test this idea, inflammation was induced in YAe62β mice by i.p. injection with LPS+αCD40 or vaccinia virus infection. Padi4-specific tT_{reg} cells expanded within the spleen in both models of inflammation whereas no significant changes in the frequency of Padi4- specific $CD4^+$ T_{conv} cells were observed (Fig. 4h–l). These data demonstrate that Padi4-specific tT_{reg} cells are exported during the neonatal window, are maintained in the peripheral repertoire and can accumulate during inflammation.

Negative selection eliminates Padi4-specific thymocytes from the adult thymus—The restricted development of Padi4-specific tT_{reg} cells to the neonatal thymus suggested mechanisms actively limit their generation in adult mice. To probe this question, we first quantified the frequency at which Padi4-specific thymocyte are present at different thymic developmental stages, in neonate and adult mice, which do or do not express endogenous Padi4. Pre-selection $CD4^+CD8^+$ (DP) $TCRβ^{int}$ $CCR7^{lo}$ thymocytes that undergo positive selection on MHC-II molecules upregulate TCRβ and CCR7 expression, and down regulate CD8 expression to become a CD4SP. Within the CD4SP compartment, thymocytes can be further delineated based on maturation status: semi-mature (SM), mature 1 (M1) and mature 2 (M2)[9, 10, 24]. Within the neonatal and adult thymus, a very small fraction of DP $TCRβ^{hi}$ $CCR7^{pos}$ thymocytes express Foxp3[25], with larger frequencies occurring at the CD4SP M1 and M2 stages (Fig. 5a,b Supplementary Fig. 4).

Within the neonatal thymus, a small fraction of Padi4-specific thymocytes begin to express Foxp3 at the CD4SP M1 stage (Fig. 5a, top row). At the CD4SP M1 stage, a significant decrease in $Foxp3^{neg}$ Padi4-specific thymocytes is also observed, in comparison to $Padi4^{-/-}$ mice (Fig. 5c–e). The increase in Padi4-specific tT_{reg} cells and decrease in $Foxp3^{neg}$ CD4SP is magnified at the CD4SP M2 stage. In adult mice, negative selection depletes Padi4-specific thymocytes beginning at the DP stage (Fig. 5b,f-h). This largely eliminates Padi4-specific thymocytes prior to upregulating TCRβ and CCR7 expression, or downregulating CD8 in $Padi4^{+/+}$ but not $Padi4^{-/-}$ mice (Fig. 5b–h, Supplementary Fig. 4). The development of Add2-specific CD4SP is similarly abrogated in adult thymus (Supplementary Fig. 4k–o). These data argue that the thymocyte stage at which Padi4-specific thymocytes recognize cognate self-antigen changes between the neonate and adult thymus.

Limiting Padi4 expression to radioresistant cells allows for adult tT_{reg} development—Mixed $Padi4^{+/+}$ and $Padi4^{-/-}$ bone marrow (BM) chimeric mice were generated to reveal the cellular sources of Padi4 that control negative selection in adult mice. Donor $Padi4^{-/-}$ BM into $Padi4^{-/-}$ mice (KO -> KO) and $Padi4^{+/+}$ BM into $Padi4^{+/+}$ mice (WT -> WT) phenocopy their parental strains; $Padi4$ deficiency in both the BM and recipient radioresistant compartments resulted in the generation of a high frequency of Padi4-specific

CD4SP thymocytes, whereas mice sufficient in Padi4 in both compartments demonstrated profound deletion at the TCRβ[int] CCR7^{neg} DP to TCRb[hi] CCR7^{pos} CD4SP transition (Fig. 6a–h). Further, neither KO -> KO or WT -> WT BM chimeric mice generated significant populations of Padi4-specific tT$_{reg}$ cells (Fig. 6i,j). The exclusive expression of Padi4 in BM cells (WT -> KO) showed a significant elimination of Padi4-specific thymocytes at the DP to CD4SP transition, and minimal development of tT$_{reg}$ cells (Fig. 6a–j). Consistent with these data, flow sorted thymic CD11c^{+} Xcr1^{neg} cDC (migratory Sirpa cDC[26]) presents IA[b]-Padi4 to T cell hybridomas (Fig. 6k,l).

Exclusive expression of Padi4 in radioresistant cells result in a partial rescue of Padi4-specific T cell development. In *Padi4*^{−/−} BM into *Padi4*^{+/+} mice (KO -> WT), significantly more Padi4-specific CCR7^{pos} TCRβ[hi] CD4SP thymocytes are generate, as compared to mice that express Padi4 in both compartments (Fig. 6a–h). Further, the elimination of Padi4 expression in BM-derived cells resulted in the differentiation of Padi4-specific CD4SP cells into tT$_{reg}$ cells (Fig. 6i,j). These data argue within the adult thymus, Padi4-expression in adult thymic stromal cells is sufficient to generate Padi4-specific tT$_{reg}$ cells, however, BM derived cells present IA[b]-Padi4 to developing thymocytes in a manner sufficient to induce negative selection at the DP to CD4SP transition.

Neonatal Padi4-specific tT$_{reg}$ cells express TCRs with modest dwell-times—

The neonatal development of Padi4-reactive tT$_{reg}$ cells and CD4^{+} T$_{conv}$ cells, as well as the overall depletion of Foxp3^{neg} M1 and M2 CD4SP cells, suggests thymocytes expressing Padi4-reactive TCRs are under selection pressures. To identify and characterize TCRs expressed on Padi4-specific thymocytes that audition for selection into the neonatal tT$_{reg}$ repertoire, IA[b]-Padi4 tetramer[pos] Foxp3-GFP[neg] CD4SP thymocytes were FACS sorted from 2-week old YAe62β mice, and eight novel TCRs were cloned (Fig. 7a,b). *In vitro* activation assays of T cell hybridomas expressing these TCRs showed a ~10^5-fold range of EC$_{50}$ values to the Padi4$_{92–105}$ epitope (Fig. 7c, Supplementary Table 2).

To reveal the fate of thymocytes expressing Padi4-reactive TCR clonotypes, TCRα deep sequencing of thymic and splenic T cell subsets isolated from YAe62β mice was performed. These experiments were used to determined the frequency at which each Padi4-reactive TCR clonotype is carried in different T cell repertoires of neonatal mice: thymic Foxp3-GFP^{neg} CD4SP, and splenic CD25^{+} Foxp3-GFP^{+} tT$_{reg}$ cells and CD4^{+} T$_{conv}$ cells (Fig. 7 d–f). Three mature T cell lineage biases were observed. Lymphocytes expressing the most potent TCRs (colored red) were largely absent from the neonatal tT$_{reg}$ and CD4^{+} T$_{conv}$ cell repertoires (Fig. 7e, f). The Padi4-reactive tT$_{reg}$ repertoire is predominately comprised of T cell clonotypes that have moderate potency (colored green), whereas the Padi4-reactive CD4^{+} T$_{conv}$ cell repertoire is primarily lymphocytes expressing TCRs with weak potency (colored blue) (Fig. 7e,f). Frequency bias into the tT$_{reg}$ or T$_{conv}$ cell repertoires ranged from 10–1,000-fold (Fig. 7g).

We next evaluated whether the observed T cell lineage biases were associated with a particular parameter of the TCR:IA[b]-Padi4 binding reaction. Surface plasmon resonance (SPR) analyses determined that the equilibrium affinity (K$_D$) of this collection of Padi4-specific TCRs ranged from 3–90 μM, and the half-life (t$_{1/2}$) or dwell time of the interactions

ranged from ~0.2–7 sec (Supplementary Table 2, Supplementary Fig. 5). Centered second order non-linear regression analysis was carried out to test whether tT_{reg}/CD4 T_{conv} cell selection bias best correlated with the TCR:self-MHC (a) half-life, $t_{1/2}$ (b) equilibrium affinity, K_D (c) on-rate, k_{on} or (d) the clonotype frequency in thymic Foxp3^{neg} CD4SP repertoire. Best probable curve fits show that the $t_{1/2}$ is the best correlate for predicting tT_{reg} development (Fig. 7h–k).

Padi4-specific TCRs that promoted neonatal tT_{reg} development ranged from ~0.8–1.4 seconds. TCRs that induce neonatal negative selection have $t_{1/2}$ of 4–7sec, whereas the $t_{1/2}$ of TCRs that The CD4+ T_{conv} cell repertoire express TCRs with very short $t_{1/2}$ (Fig. 7l–n). A similar ordering occurs when kinetic values are used to estimate the confinement time (t_a) of the TCR:pMHC interaction (Supplementary Table 2)[27, 28]. In contrast, Padi4-specific TCRs with K_D values of 8–20μM promoted negative selection (TCR 5290), biased towards the tT_{reg} repertoire (TCRs 4699, 4738, 5292 and 6239) or were enriched in the CD4 T_{conv} cell lineage (6236 and 6256). Consistent with these data, the Add2$_{606–621}$-reactive 6287 tT_{reg} TCR has a K_D of ~40μM and $t_{1/2}$ ~0.9sec. These data argue that TCR:self-pMHC dwell time forms a kinetic window that promotes the generation of neonatal Padi4-specific tT_{reg} cells.

Padi4-specific tT_{reg} TCRs use conventional TCR:pMHC docking orientations.

—To identify in molecular detail how TCRs that regulate neonatal thymocyte fate choice bind their self-ligands, we determined the crystal structures of six TCRs bound to IA[b]-Padi4$_{92–105}$. The set includes two TCRs that induce neonatal negative selection (TCRs 6235 and 5287), or promoted the development of neonatal tT_{reg} cells (TCRs 4699 and 4738) or CD4+ T_{conv} cells (TCRs 6256 and 6236) (Fig. 8a–c, Supplementary Fig. 6). The resolutions of the TCR:pMHC complexes range from 2.7 – 3.4 Å (Supplementary Table 3). The overall buried surface area (BSA) of the complexes range from 1440–1500 Å^2, with ~60% of the BSA derived from TCR:IA[b]α chain interactions (Fig. 8d–i, Supplementary Fig. 6). Each of the TCRs binds IA[b]-Padi4 using a conventional TCR:pMHC orientation, with crossing angles of 41–46° and incident angles of 13–15° (Fig. 8j,k).

Within the set, the 6235, 4699 and 6256 TCRs differ only at a single CDR3α residue (TCRα 94 E, D and A, respectively). This high degree of sequence homology allowed for detailed assessment of structural features that regulate TCR:self-pMHC binding kinetics, and ultimately neonatal thymocytes fate choice. Overall, the TCR and pMHC residues that form the binding interface and BSA are nearly identical. The most noteworthy alterations in the binding interface occur between the CDR3α 94 residue and the hydroxyl moiety of the Padi4 peptide P2 tyrosine (p2Y) (Fig. 8l–n). The 6235 CDR3α 94E residue contacts include a hydrogen bond with a length of 2.2Å, whereas the electrostatic interactions between the 4699 CDR3α 94D residue is at a less ideal distance of 2.7Å (Fig. 8o,p). The 6256 CDR3α 94A residue does not interact with the P2Y residue, with only the CDR1α 28 residue forming a van der Waals contact with the hydroxyl of the p2Y (Fig. 8n,q).

To test whether the Padi4 p2Y hydroxyl is the lynchpin controlling the differences in dwell times, SPR analyses of the three TCRs binding IA[b]-Padi4 carrying a phenylalanine at p2 (p2F) was performed. The 6235, 4699 and 6256 TCRs bind IA[b]-Padi4 with $t_{1/2}$ of 5, 1.4 and 0.4 sec, respectively (Fig. 8r, Supplementary Table 2). In contrast, the three TCRs bound

IA^b-Padi4 p2F with near identical binding kinetics, including a more rapid $t_{1/2}$ of ~0.2sec (Fig. 8s). Thus, unique interactions created between the 6235, 4699 and 6256 TCRα chains with the IA^b-Padi4 p2Y hydroxyl manifest differences in the TCR:self-pMHC dwell times, which allows the 4699 TCR to bias thymocytes into the neonatal tT$_{reg}$ repertoire.

Discussion

Despite the critical nature of neonate-derived tT$_{reg}$ cells in establishing immune homeostasis, the ligand specificities of this T cell repertoire are largely unexplored. Here we identified self-ligands recognized by neonatal tT$_{reg}$ cells, and elucidated ligand recognition parameters that promote tT$_{reg}$ differentiation. Within the neonatal thymus, Padi4-specific thymocytes have a fate choice at the CD4SP stage: develop into tT$_{reg}$ or CD4 T$_{conv}$ cells, or undergo deletion. Our results argue that the outcome of this selection branch point is clonotype specific, and predicated on the dwell time of the TCR:self-pMHC interaction. In the adult thymus, however, Padi4-reactive thymocytes undergo negative selection at the DP to CD4SP transition, precluding their ability to differentiate into CD4 T$_{conv}$ or tT$_{reg}$ cells. Our results reveal roles for temporally regulated changes in negative selection and TCR:self-pMHC kinetics in framing the neonatal tT$_{reg}$ selection window.

TCR-centric hypotheses have been proposed to account for the ability of self-reactive thymocytes to escape negative selection and be exported as tT$_{reg}$ cells or autoimmune T$_{conv}$ cells. One model, named the "hit and run" hypothesis, argues that the Foxp3 program results from altered or attenuated agonist TCR signals, which are insufficient to induce clonal deletion[5]. Attenuated TCR signals may arise from thymocytes recognizing low abundant thymic self-peptides or rare APCs that present them[5, 12]. This model arose, in part, to explain several aspects of tT$_{reg}$ development. Reporter models of TCR signaling, TCRβ chain usage and certain TCR-cognate self-ligand models argue that thymocytes interactions with agonist self-pMHC promote tT$_{reg}$ development, and that the tT$_{reg}$ repertoire carries increased self-reactivity, relative to the CD4 T$_{conv}$ cell repertoire[5, 17, 20, 29–35]. However, agonist selection of tT$_{reg}$ cells has not been uniformly observed[36, 37]. Further, the TCR repertoires of CD4$^+$ T$_{conv}$ cells and Foxp3$^+$ T$_{reg}$ cells display some clonotype overlap[38], which may result from a broad range of TCR affinities being able to induce tT$_{reg}$ cell development[39]. Our observation that TCR:self-pMHC dwell time is a key variable in determining the outcome of neonatal T cell development is consistent with the 'hit and run' model, as TCR signal quality can be dependent upon TCR:pMHC binding kinetics[40].

Non-canonical TCR docking on pMHC can result in the generation of abnormal TCR signal transduction events,[41, 42], which may arise from altered TCR synapse formation and recruitment of co-stimulatory molecules[43]. How frequently altered binding modes are used by self-reactive thymocytes to escape negative selection is unclear, though the lone report of human induced T$_{reg}$ TCRs bound to pMHC revealed a reversed binding polarity[44]. In the examples presented here, the TCR:pMHC docking orientation was found to be within published examples of TCRs expressed by conventional foreign-reactive MHC-I and MHC-II restricted T cells. Nevertheless, the ~1–2sec dwell times used by Padi4-reactive tT$_{reg}$ cells are shorter than most T cells responding to pathogen challenge[45], which may limit or alter

certain aspects of TCR signaling and subsequent gene transcription during neonatal T cell development.

Thymocyte extrinsic factors contribute to the ability of tT$_{reg}$ cells and autoimmune CD4 T cells to develop. Cytokine availability and antigenic niches limit the total number of tT$_{reg}$ cells and the frequency of individual clonotypes[2, 46]. As mice age, peripheral mature Foxp3$^+$ tT$_{reg}$ cells recirculate to the thymus, and limit the production of adult-selected tT$_{reg}$ cells by limiting IL-2 but not necessarily TCR signaling[47, 48]. Our observation that the TCR:self-pMHC dwell time correlates with thymic selection outcome supports the hypothesis that competitive forces manifest on individual clonotypes, and not necessarily between different clonotypes that recognize the same self-antigen.

Maturation of the thymus from the perinate and neonate ages to adult includes changes to thymic APC populations. The maturation process includes the seeding of the thymus with migratory DC populations, and changes in MHC-II antigen processing machinery within medullary epithelial cells[4, 26]. These processes can influence tT$_{reg}$ selection, and provide a window in which pathogenic T$_{conv}$ cells can more efficiently develop[49]. Closing the temporal window of Padi4-specific tT$_{reg}$ development involves a thymocyte stage-specific switch in antigen recognition, which results in negative selection of adult Padi4-specific thymocytes at the DP to CD4SP transition. Deletion in the adult thymus occurs prior to upregulating CCR7, a chemokine receptor that promotes thymocyte migration from the cortex to medulla[8], suggesting cortical residency. The dichotomy of neonate versus adult selection of Padi4-specific T cell development outcomes occurs despite studies showing that negative selection to ubiquitously expressed antigens is fully functional during the neonatal period[4, 50]. Our data argue that age-dependent changes in negative selection constrict the development of certain tT$_{reg}$ specificities to the neonatal thymus.

Supplementary Material

Refer to Web version on PubMed Central for supplementary material.

Acknowledgments

References

1. Hogquist KA, Jameson SC. The self-obsession of T cells: how TCR signaling thresholds affect fate 'decisions' and effector function. Nat Immunol 2014, 15(9): 815–823. [PubMed: 25137456]

2. Klein L, Robey EA, Hsieh CS. Central CD4(+) T cell tolerance: deletion versus regulatory T cell differentiation. Nat Rev Immunol 2019, 19(1): 7–18. [PubMed: 30420705]

3. Sakaguchi S, Yamaguchi T, Nomura T, Ono M. Regulatory T cells and immune tolerance. Cell 2008, 133(5): 775–787. [PubMed: 18510923]

4. Yang S, Fujikado N, Kolodin D, Benoist C, Mathis D. Immune tolerance. Regulatory T cells generated early in life play a distinct role in maintaining self-tolerance. Science 2015, 348(6234): 589–594. [PubMed: 25791085]

5. Li MO, Rudensky AY. T cell receptor signalling in the control of regulatory T cell differentiation and function. Nat Rev Immunol 2016, 16(4): 220–233. [PubMed: 27026074]

6. Mathis D, Benoist C. Aire. Annu Rev Immunol 2009, 27: 287–312. [PubMed: 19302042]

7. Takaba H, Morishita Y, Tomofuji Y, Danks L, Nitta T, Komatsu N, et al. Fezf2 Orchestrates a Thymic Program of Self-Antigen Expression for Immune Tolerance. Cell 2015, 163(4): 975–987. [PubMed: 26544942]

8. Takahama Y. Journey through the thymus: stromal guides for T-cell development and selection. Nat Rev Immunol 2006, 6(2): 127–135. [PubMed: 16491137]

9. Daley SR, Hu DY, Goodnow CC. Helios marks strongly autoreactive CD4+ T cells in two major waves of thymic deletion distinguished by induction of PD-1 or NF-kappaB. J Exp Med 2013, 210(2): 269–285. [PubMed: 23337809]

10. Cowan JE, Parnell SM, Nakamura K, Caamano JH, Lane PJ, Jenkinson EJ, et al. The thymic medulla is required for Foxp3+ regulatory but not conventional CD4+ thymocyte development. J Exp Med 2013, 210(4): 675–681. [PubMed: 23530124]

11. Kishimoto H, Sprent J. Negative selection in the thymus includes semimature T cells. J Exp Med 1997, 185(2): 263–271. [PubMed: 9016875]

12. Weissler KA, Caton AJ. The role of T-cell receptor recognition of peptide:MHC complexes in the formation and activity of Foxp3(+) regulatory T cells. Immunol Rev 2014, 259(1): 11–22. [PubMed: 24712456]

13. Malchow S, Leventhal DS, Nishi S, Fischer BI, Shen L, Paner GP, et al. Aire-dependent thymic development of tumor-associated regulatory T cells. Science 2013, 339(6124): 1219–1224. [PubMed: 23471412]

14. Perry JSA, Lio CJ, Kau AL, Nutsch K, Yang Z, Gordon JI, et al. Distinct contributions of Aire and antigen-presenting-cell subsets to the generation of self-tolerance in the thymus. Immunity 2014, 41(3): 414–426. [PubMed: 25220213]

15. Guerau-de-Arellano M, Martinic M, Benoist C, Mathis D. Neonatal tolerance revisited: a perinatal window for Aire control of autoimmunity. J Exp Med 2009, 206(6): 1245–1252. [PubMed: 19487417]

16. Gratz IK, Campbell DJ. Organ-specific and memory treg cells: specificity, development, function, and maintenance. Front Immunol 2014, 5: 333. [PubMed: 25076948]

17. Leonard JD, Gilmore DC, Dileepan T, Nawrocka WI, Chao JL, Schoenbach MH, et al. Identification of Natural Regulatory T Cell Epitopes Reveals Convergence on a Dominant Autoantigen. Immunity 2017, 47(1): 107–117 e108. [PubMed: 28709804]

18. Spence A, Purtha W, Tam J, Dong S, Kim Y, Ju CH, et al. Revealing the specificity of regulatory T cells in murine autoimmune diabetes. Proc Natl Acad Sci U S A 2018, 115(20): 5265–5270. [PubMed: 29712852]

19. Liu X, Nguyen P, Liu W, Cheng C, Steeves M, Obenauer JC, et al. T cell receptor CDR3 sequence but not recognition characteristics distinguish autoreactive effector and Foxp3(+) regulatory T cells. Immunity 2009, 31(6): 909–920. [PubMed: 20005134]

20. Kieback E, Hilgenberg E, Stervbo U, Lampropoulou V, Shen P, Bunse M, et al. Thymus-Derived Regulatory T Cells Are Positively Selected on Natural Self-Antigen through Cognate Interactions of High Functional Avidity. Immunity 2016, 44(5): 1114–1126. [PubMed: 27192577]

21. Malhotra D, Linehan JL, Dileepan T, Lee YJ, Purtha WE, Lu JV, et al. Tolerance is established in polyclonal CD4(+) T cells by distinct mechanisms, according to self-peptide expression patterns. Nat Immunol 2016, 17(2): 187–195. [PubMed: 26726812]

22. Leventhal DS, Gilmore DC, Berger JM, Nishi S, Lee V, Malchow S, et al. Dendritic Cells Coordinate the Development and Homeostasis of Organ-Specific Regulatory T Cells. Immunity 2016, 44(4): 847–859. [PubMed: 27037189]

23. Kalekar LA, Schmiel SE, Nandiwada SL, Lam WY, Barsness LO, Zhang N, et al. CD4(+) T cell anergy prevents autoimmunity and generates regulatory T cell precursors. Nat Immunol 2016, 17(3): 304–314. [PubMed: 26829766]

24. Xing Y, Wang X, Jameson SC, Hogquist KA. Late stages of T cell maturation in the thymus involve NF-kappaB and tonic type I interferon signaling. Nat Immunol 2016, 17(5): 565–573. [PubMed: 27043411]

25. Fontenot JD, Dooley JL, Farr AG, Rudensky AY. Developmental regulation of Foxp3 expression during ontogeny. J Exp Med 2005, 202(7): 901–906. [PubMed: 16203863]

26. Li J, Park J, Foss D, Goldschneider I. Thymus-homing peripheral dendritic cells constitute two of the three major subsets of dendritic cells in the steady-state thymus. J Exp Med 2009, 206(3): 607–622. [PubMed: 19273629]

27. Govern CC, Paczosa MK, Chakraborty AK, Huseby ES. Fast on-rates allow short dwell time ligands to activate T cells. Proc Natl Acad Sci U S A 2010, 107(19): 8724–8729. [PubMed: 20421471]

28. Aleksic M, Dushek O, Zhang H, Shenderov E, Chen JL, Cerundolo V, et al. Dependence of T cell antigen recognition on T cell receptor-peptide MHC confinement time. Immunity 2010, 32(2): 163–174. [PubMed: 20137987]

29. Jordan MS, Boesteanu A, Reed AJ, Petrone AL, Holenbeck AE, Lerman MA, et al. Thymic selection of CD4+CD25+ regulatory T cells induced by an agonist self-peptide. Nat Immunol 2001, 2(4): 301–306. [PubMed: 11276200]

30. Apostolou I, Sarukhan A, Klein L, von Boehmer H. Origin of regulatory T cells with known specificity for antigen. Nat Immunol 2002, 3(8): 756–763. [PubMed: 12089509]

31. Aschenbrenner K, D'Cruz LM, Vollmann EH, Hinterberger M, Emmerich J, Swee LK, et al. Selection of Foxp3+ regulatory T cells specific for self antigen expressed and presented by Aire+ medullary thymic epithelial cells. Nat Immunol 2007, 8(4): 351–358. [PubMed: 17322887]

32. Legoux FP, Lim JB, Cauley AW, Dikiy S, Ertelt J, Mariani TJ, et al. CD4+ T Cell Tolerance to Tissue-Restricted Self Antigens Is Mediated by Antigen-Specific Regulatory T Cells Rather Than Deletion. Immunity 2015, 43(5): 896–908. [PubMed: 26572061]

33. Barthlott T, Kassiotis G, Stockinger B. T cell regulation as a side effect of homeostasis and competition. J Exp Med 2003, 197(4): 451–460. [PubMed: 12591903]

34. Moran AE, Holzapfel KL, Xing Y, Cunningham NR, Maltzman JS, Punt J, et al. T cell receptor signal strength in Treg and iNKT cell development demonstrated by a novel fluorescent reporter mouse. J Exp Med 2011, 208(6): 1279–1289. [PubMed: 21606508]

35. Stadinski BD, Shekhar K, Gomez-Tourino I, Jung J, Sasaki K, Sewell AK, et al. Hydrophobic CDR3 residues promote the development of self-reactive T cells. Nat Immunol 2016, 17(8): 946–955. [PubMed: 27348411]

36. van Santen HM, Benoist C, Mathis D. Number of T reg cells that differentiate does not increase upon encounter of agonist ligand on thymic epithelial cells. J Exp Med 2004, 200(10): 1221–1230. [PubMed: 15534371]

37. Pacholczyk R, Kern J, Singh N, Iwashima M, Kraj P, Ignatowicz L. Nonself-antigens are the cognate specificities of Foxp3+ regulatory T cells. Immunity 2007, 27(3): 493–504. [PubMed: 17869133]

38. Hsieh CS, Zheng Y, Liang Y, Fontenot JD, Rudensky AY. An intersection between the self-reactive regulatory and nonregulatory T cell receptor repertoires. Nat Immunol 2006, 7(4): 401–410. [PubMed: 16532000]

39. Lee HM, Bautista JL, Scott-Browne J, Mohan JF, Hsieh CS. A broad range of self-reactivity drives thymic regulatory T cell selection to limit responses to self. Immunity 2012, 37(3): 475–486. [PubMed: 22921379]

40. Andreotti AH, Joseph RE, Conley JM, Iwasa J, Berg LJ. Multidomain Control Over TEC Kinase Activation State Tunes the T Cell Response. Annu Rev Immunol 2018, 36: 549–578. [PubMed: 29677469]

41. Hahn M, Nicholson MJ, Pyrdol J, Wucherpfennig KW. Unconventional topology of self peptide-major histocompatibility complex binding by a human autoimmune T cell receptor. Nat Immunol 2005, 6(5): 490–496. [PubMed: 15821740]

42. Adams JJ, Narayanan S, Liu B, Birnbaum ME, Kruse AC, Bowerman NA, et al. T cell receptor signaling is limited by docking geometry to peptide-major histocompatibility complex. Immunity 2011, 35(5): 681–693. [PubMed: 22101157]

43. Schubert DA, Gordo S, Sabatino JJ Jr., Vardhana S, Gagnon E, Sethi DK, et al. Self-reactive human CD4 T cell clones form unusual immunological synapses. J Exp Med 2012, 209(2): 335–352. [PubMed: 22312112]

44. Beringer DX, Kleijwegt FS, Wiede F, van der Slik AR, Loh KL, Petersen J, et al. T cell receptor reversed polarity recognition of a self-antigen major histocompatibility complex. Nat Immunol 2015.

45. Altan-Bonnet G, Germain RN. Modeling T cell antigen discrimination based on feedback control of digital ERK responses. PLoS Biol 2005, 3(11): e356. [PubMed: 16231973]

46. Bautista JL, Lio CW, Lathrop SK, Forbush K, Liang Y, Luo J, et al. Intraclonal competition limits the fate determination of regulatory T cells in the thymus. Nat Immunol 2009, 10(6): 610–617. [PubMed: 19430476]

47. Thiault N, Darrigues J, Adoue V, Gros M, Binet B, Perals C, et al. Peripheral regulatory T lymphocytes recirculating to the thymus suppress the development of their precursors. Nat Immunol 2015, 16(6): 628–634. [PubMed: 25939024]

48. Weist BM, Kurd N, Boussier J, Chan SW, Robey EA. Thymic regulatory T cell niche size is dictated by limiting IL-2 from antigen-bearing dendritic cells and feedback competition. Nat Immunol 2015, 16(6): 635–641. [PubMed: 25939026]

49. Huseby ES, Sather B, Huseby PG, Goverman J. Age-dependent T cell tolerance and autoimmunity to myelin basic protein. Immunity 2001, 14(4): 471–481. [PubMed: 11336692]

50. Dong M, Artusa P, Kelly SA, Fournier M, Baldwin TA, Mandl JN, et al. Alterations in the Thymic Selection Threshold Skew the Self-Reactivity of the TCR Repertoire in Neonates. J Immunol 2017, 199(3): 965–973. [PubMed: 28659353]
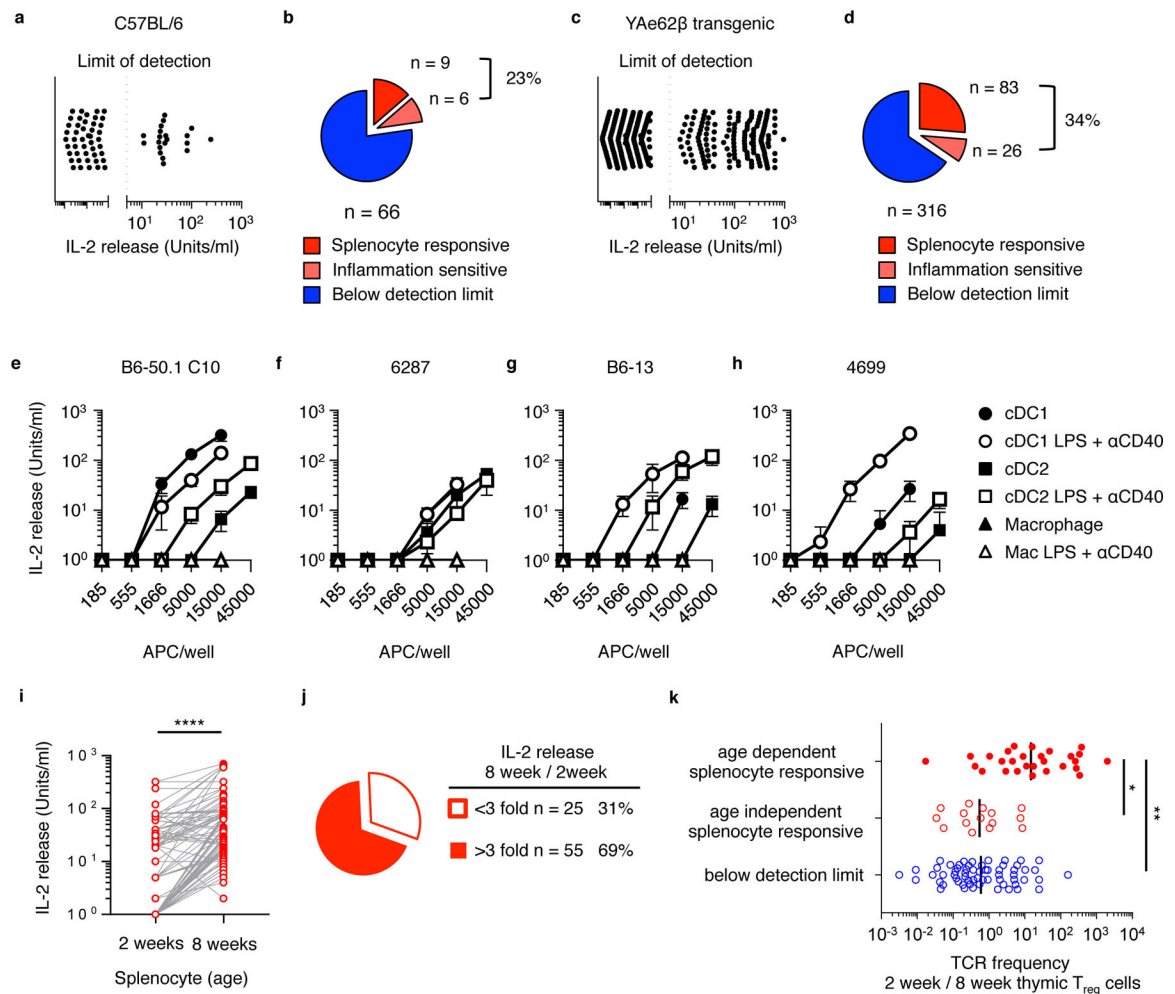
Figure 1.

T cell receptors expressed on neonate-derived tT_{reg} cells can recognize steady state, inflammation- and age-dependent self-antigens. (**a**) IL-2 release and (**b**) frequency at which 66 C57BL/6-derived tT_{reg} hybridomas and (**c, d**) 316 Yae62β^+ tT_{reg} hybridomas react with splenocytes isolated from adult naïve mice (red) or mice pretreated with LPS and αCD40 (pink). (**e**) IL-2 response of B6–50.1C10, (**f**) 6287, (**g**) B6–13 and (**h**) 4699 tT_{reg} hybridomas cultured with titrating numbers of cDC1, cDC2 and macrophages isolated from naïve mice (filled symbol) or mice pretreated with LPS and αCD40 (open symbol). Data are an example of three independent experiments giving similar results. Error bars show standard deviation. (**i**) IL-2 release by 80 *in vitro* splenocyte-reactive tT_{reg} hybridomas cultured with spleen cells isolated from 2 week old and 8 week old C57BL/6 mice. Results are from two independent experiments with similar results. (**j**) Quantification of splenocyte-reactive hybridomas that increase IL-2 production in response to adult v. neonatal spleen cells. (**k**) The frequency of age-dependent (red, filled circles), age-independent *in vitro* splenocyte-responsive (red, open circles) and below detection limit (blue) TRAV14$^+$ (Vα2$^+$) tT_{reg} TCRs carried in the thymic Foxp3$^+$ tT_{reg} pool at 2 weeks of age as compared to 8 weeks of age. Lines represent the data geometric mean. Data are from (**i,j**) 80 self-reactive and (**k**) 103 Vα2$^+$ clonotypes; 28 age-dependent, 12 age-independent and 63 below limit of detection. (i)
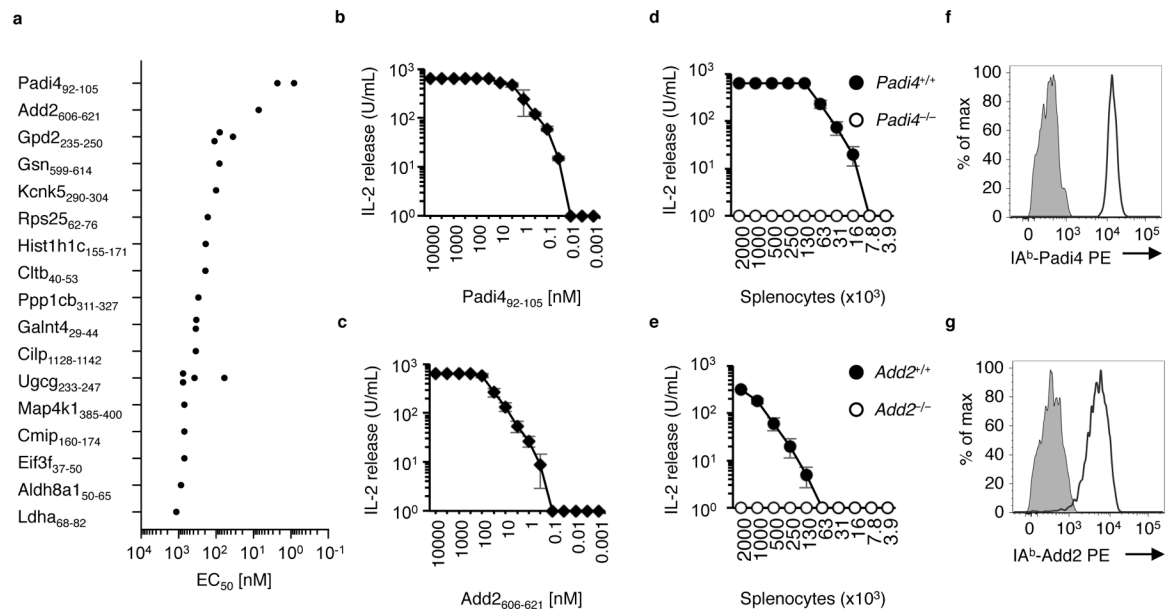
****P<0.0001 ratio paired 2-tailed t test, (k) *P<0.05, **P<0.01 one-way ANOVA Tukey multiple comparisons test.
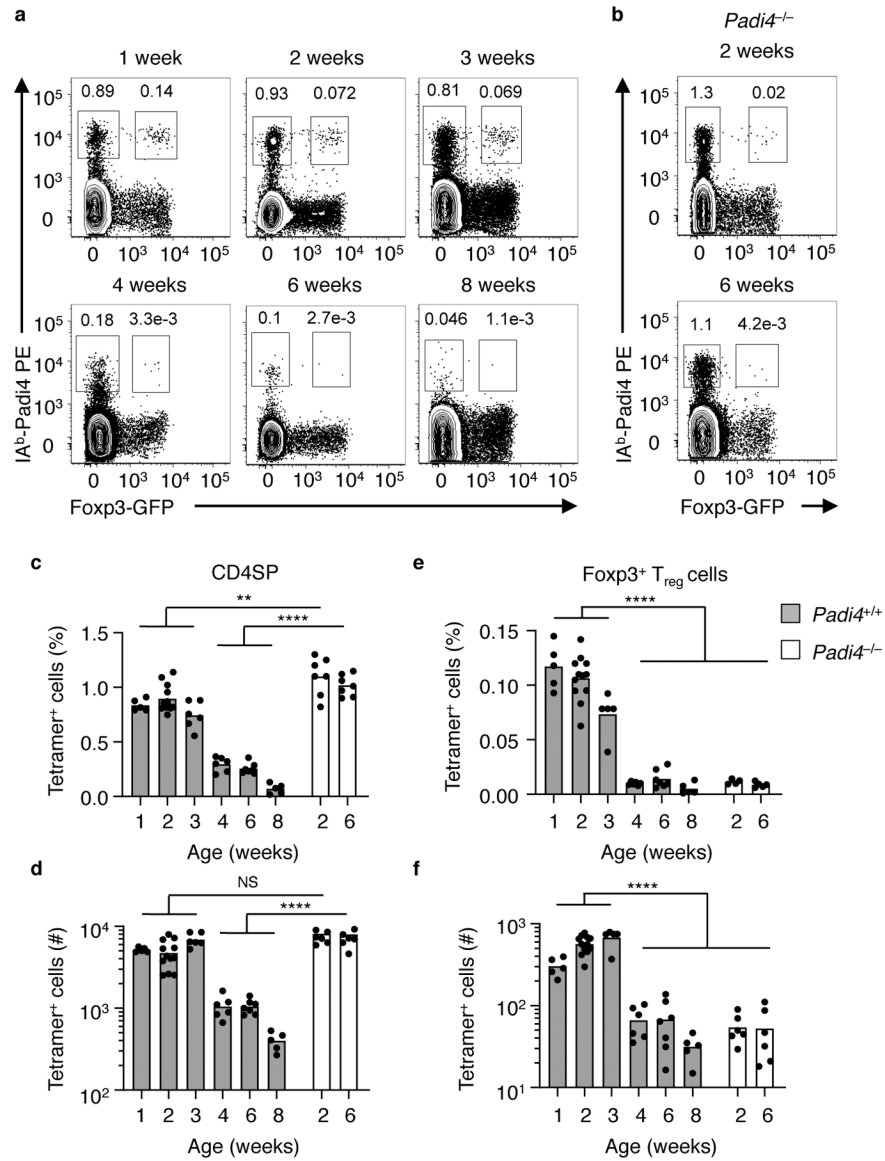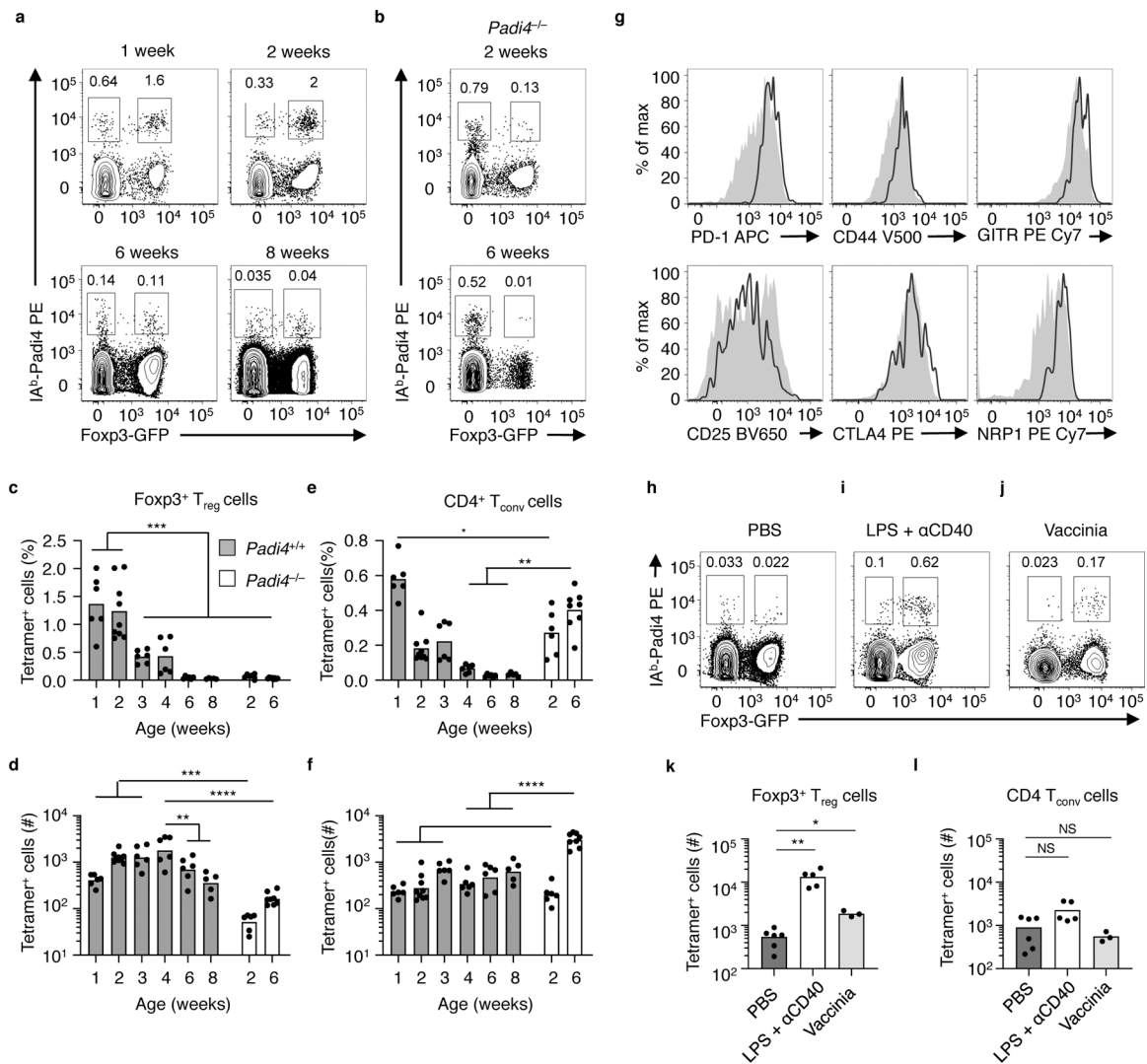
Figure 2.

Identification of self-ligands recognized by neonatal tT_{reg} TCR using an immunopeptidome library screen. (**a**) Chart of EC_{50} values of IL-2 release for tT_{reg} hybridomas responding to titrating concentrations of library-identified self-peptides. (**b-e**) IL-2 release of the (**b**) 4699 tT_{reg} hybridoma and (**c**) 6287 4699 tT_{reg} hybridoma cultured with titrating concentrations of identified $Padi4_{92–105}$ or $Add2_{606–621}$ presented by IA^b expressing mouse fibroblasts, or (**d**) with titrating concentrations of C57BL/6 or $Padi4^{-/-}$ splenocytes, or (**e**) with titrating concentrations of C57BL/6 or $Add2^{-/-}$ splenocytes. Data are example of three independent experiments giving similar results. Error bars show standard deviation. (**f**) IA^b-Padi4 tetramer staining of the 4699 tT_{reg} hybridoma, and (**g**) IA^b-Add2 tetramer staining of the 6287 tT_{reg} hybridoma (black line). Gray negative control stains are the IA^b-Add2 tetramer staining of the 4699 tT_{reg} hybridoma and the IA^b-Padi4 tetramer staining the 6287 tT_{reg} hybridoma.

Figure 3.
Development of Padi4$_{92-105}$-specific tT$_{reg}$ cells is restricted to the neonatal thymus. (**a**, **b**) Flow cytometry of Vα2$^+$ CD4$^+$CD8$^-$ thymocytes in (**a**) YAe62β.*Foxp3-GFP* and (**b**) *Padi4$^{-/-}$*.YAe62β.*Foxp3-GFP* mice at different ages; numbers adjacent to outlined areas indicate percent IA^b-Padi4 tetramer$^+$ Foxp3-GFP$^-$ (left) and Foxp3-GFP$^+$ (right). (**c-f**) Frequency and total cell numbers of IA^b-Padi4$^+$ (**c**, **d**) CD4$^+$CD8$^-$ Foxp3$^-$ and (**e**, **f**) Foxp3-GFP$^+$ tT$_{reg}$ cells in WT and *Padi4$^{-/-}$* YAe62β.*Foxp3-GFP* mice at different ages. Bars represent the data mean, n = 6, 12, 6, 6, 6, 6 WT mice at 1, 2, 3, 4, and 8 weeks old, n = 7 *Padi4$^{-/-}$* 2 and 6 weeks old. (c-f) NS P>0.05, **P<0.01, ***P<0.01, ****P<0.0001 one-way ANOVA Tukey multiple comparisons test.

Figure 4.
Padi4-specific tT$_{reg}$ cells seed the peripheral repertoire during the neonatal window and respond to inflammation. (**a, b**) Flow cytometry of splenic Vα2$^+$ CD4$^+$ T cells in (**a**) YAe62β.*Foxp3-GFP* mice and (**b**) *Padi4$^{-/-}$*.YAe62β.*Foxp3-GFP* mice at different ages (weeks). (**c-f**) Frequency and (**d**) total numbers of IA^b-Padi4 tetramer^{pos} Vα2$^+$ CD4$^+$ Foxp3-GFP^{pos} tT$_{reg}$ cells and (**e, f**) Vα2$^+$ CD4$^+$ Foxp3-GFP^{neg} CD4 T$_{conv}$ cells in YAe62β.*Foxp3-GFP* and *Padi4$^{-/-}$*.YAe62β.*Foxp3-GFP* mice at different ages. (**g**) Flow cytometry analyzing the expression of PD-1, CD44, GITR, CD25, CTLA4 and Nrp1 on IA^b-Padi4 tetramer^{pos} Vα2$^+$CD4$^+$Foxp3-GFP^{pos} tT$_{reg}$ cells isolated from 2 week old YAe62β.*Foxp3-GFP* mice (black line). Gray histograms are IA^b-Padi4 tetramer^{neg} Vα2$^+$CD4$^+$Foxp3-GFP^{pos} tT$_{reg}$ cells in the same mice. (**h-l**) Flow cytometry of Vα2$^+$ CD4$^+$ T cells isolated from 8 week old YAe62β.*Foxp3-GFP* mice following i.p. injection of (**h**) PBS, (**i**) LPS + αCD40 and (**j**) rVaccina virus 5 days prior. Quantification of IA^b-Padi4 tetramer^{pos} (**k**) CD4$^+$Foxp3-GFP^{pos} tT$_{reg}$ cells and (**l**) Foxp3-GFP^{neg} CD4 T$_{conv}$ cells present in YAe62β.*Foxp3-GFP* mice following i.p. injection of PBS, LPS+αCD40 or rVac virus. (a g) Data are derived from 3 independent experiments giving similar results, bars represent the data mean, n = 6, 9, 6, 6,

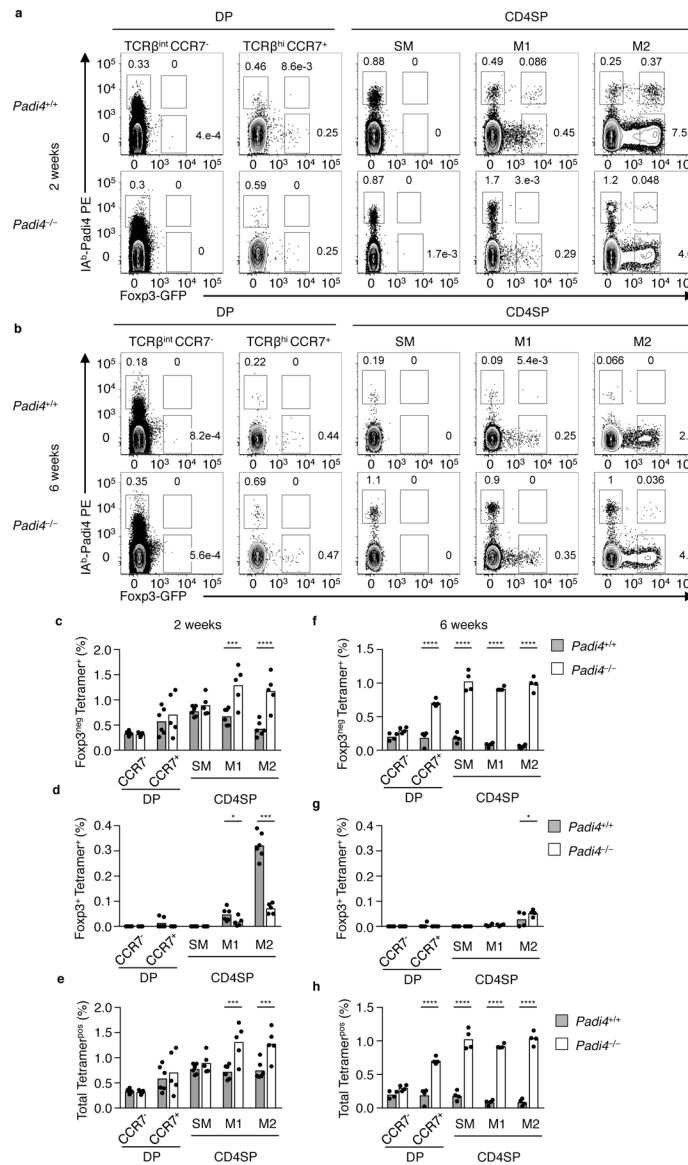6, 6 WT mice at 1, 2, 3, 4, and 8 weeks old, n = 6 and 8 *Padi4*$^{-/-}$ 2 and 6 weeks old. (h-l) Data pooled from 3 independent experiments with similar results, with 9, 5 and 6 mice per group, bars represent the data mean. Significance identified using a one-way ANOVA Tukey multiple comparisons test, and (k,l) non-parametric Dunn's multiple comparison test. ns P>0.05, *P<0.05, **P<0.01, ***P<0.001, ****P<0.0001.

Figure 5.

Padi4-specific thymocytes are subject to temporally regulated, stage-specific changes in negative selection. Flow cytometry analyses of (**a**) neonatal and (**b**) adult Vα2[+] DP and CD4SP thymocytes isolated from *Padi4^{+/+}.YAe62β.Foxp3-GFP* (top row) and *Padi4^{−/−}.YAe62β.Foxp3-GFP* (bottom row) mice for Foxp3 expression and IA[b]-Padi4 tetramer binding. Subsets shown are pre-selection DP (CD4^{+} CD8^{+} TCRβ^{int} CCR7^{neg}), post-selection DP (CD4^{+}CD8^{+} TCRβ^{hi} CCR7^{pos}), and TCRβ^{hi} CCR7^{pos} CD4SP thymocytes pre-gated on CD69^{+} MHC-I^{lo} (SM), CD69^{+} MHC-I^{hi} (M1) and CD69^{lo} MHC-I^{hi} (M2). (**c-g**) Quantification of the frequency of IA[b]-Padi4 tetramer^{pos} (**c,f**) Foxp3^{neg}, (**d,g**) Foxp3^{pos} and (**e,h**) total (Foxp3^{neg} + Foxp3^{+}) thymocytes within each thymic subset. (**c-h**) Data are derived from 3 independent experiments giving similar results, bars represent the data mean, n = 6 WT and *Padi4^{−/−}* mice at 2 and 6 weeks old. Significance identified using a one-way
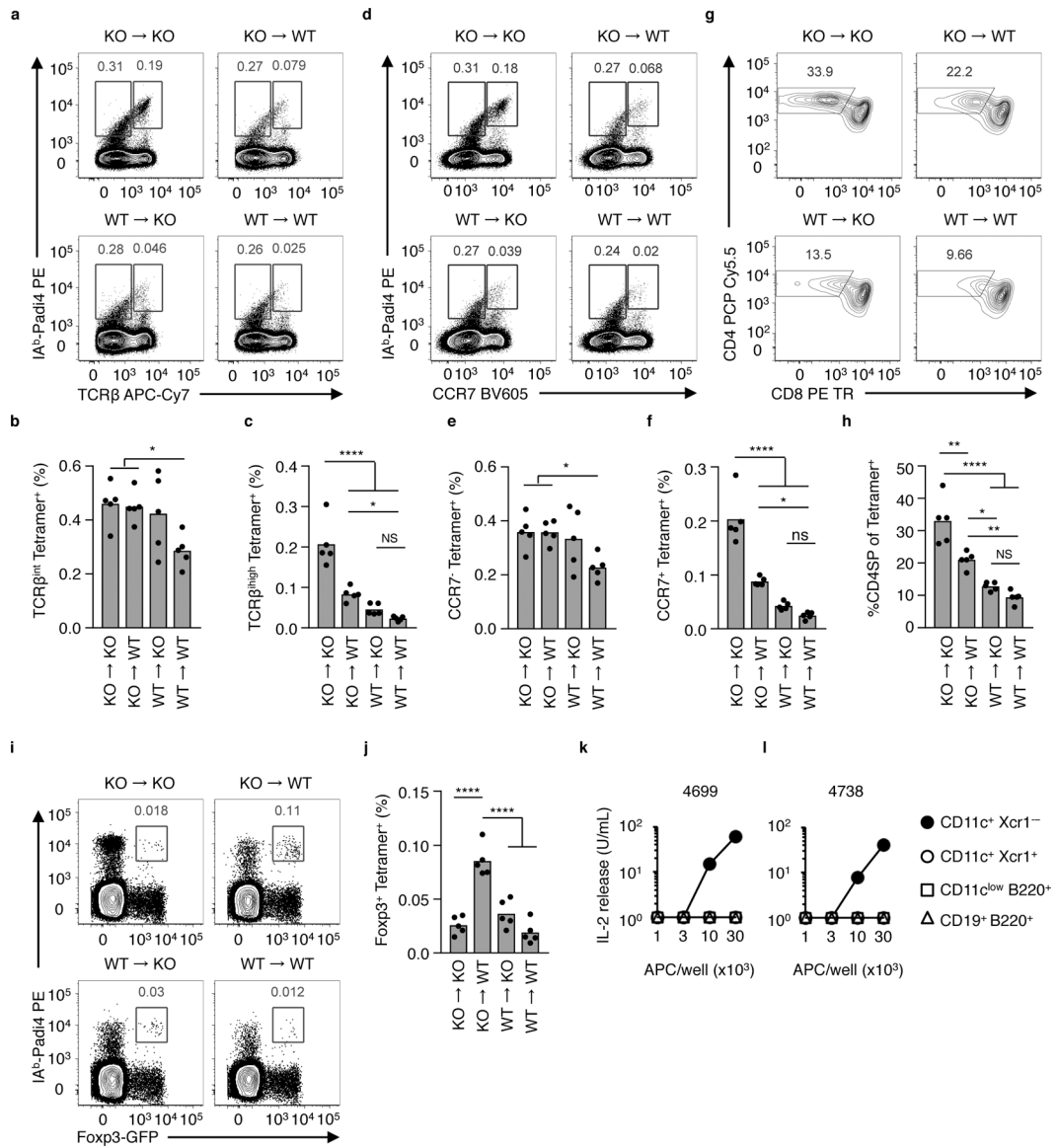
ANOVA Sidak's multiple comparison test. ns P>0.05, *P<0.05, **P<0.01, ***P<0.001, ****P<0.0001.

Figure 6.

Limiting Negative Selection restores development of Padi4-specific tT_{reg} cells in the adult thymus. (**a-j**) Eliminating Padi4 expression in BM derived cells increases the frequency of Padi4-specific $TCR\beta^{hi}$ $CCR7^+$ CD4SP thymocytes and tT_{reg} cells. Flow cytometry analyses of thymocytes isolated from mixed WT and *Padi4*$^{-/-}$ (KO) YAe62β bone marrow chimeric mice. (**a, b**) Total $V\alpha2^+$ thymocytes analyzed for IA^b-Padi4 tetramer binding and (**a**) $TCR\beta$ and (**b**) CCR7 expression. (**c**) Flow cytometry analyses of total $V\alpha2^+$ IA^b-Padi4 tetramer^{pos} thymocytes for CD4 and CD8 expression. (**d-h**) Quantification of $V\alpha2^+$ IA^b-Padi4 tetramer^{pos} (**d**) $TCR\beta^{int}$ (**e**) $TCR\beta^{hi}$ (**f**) $CCR7^{neg}$ (**g**) $CCR7^{pos}$ and (**h**) CD4SP thymocytes. (**i**) $V\alpha2^+$ CD4SP thymocytes analyzed for IA^b-Padi4 tetramer binding and Foxp3 expression, and (**j**) quantification of IA^b-Padi4 tetramer^{pos} Foxp3-GFP$^+$ CD4SP thymocytes. Data is from two independent experiments giving similar results, n = 5 mice per group, bars represent the data mean. (**k,l**) IL-2 response of the (**k**) 4699 and (**l**) 4738 tT_{reg} hybridomas

cultured with titrating numbers of CD11c$^+$ Xcr1^{neg} cDC (filled circle), CD11c$^+$ Xcr1^{pos} cDC (open circle), CD11c^{lo} B220$^+$ pDC (open squares) and CD19$^+$ B220$^+$ B cells (open triangle) isolated from thymus of adult C57BL/6 mice. Data is from two independent experiments giving similar results. Significance identified using a one-way ANOVA Tukey multiple comparisons test, ns $P>0.05$, *$P<0.05$, **$P<0.01$, ***$P<0.001$, ****$P<0.0001$.
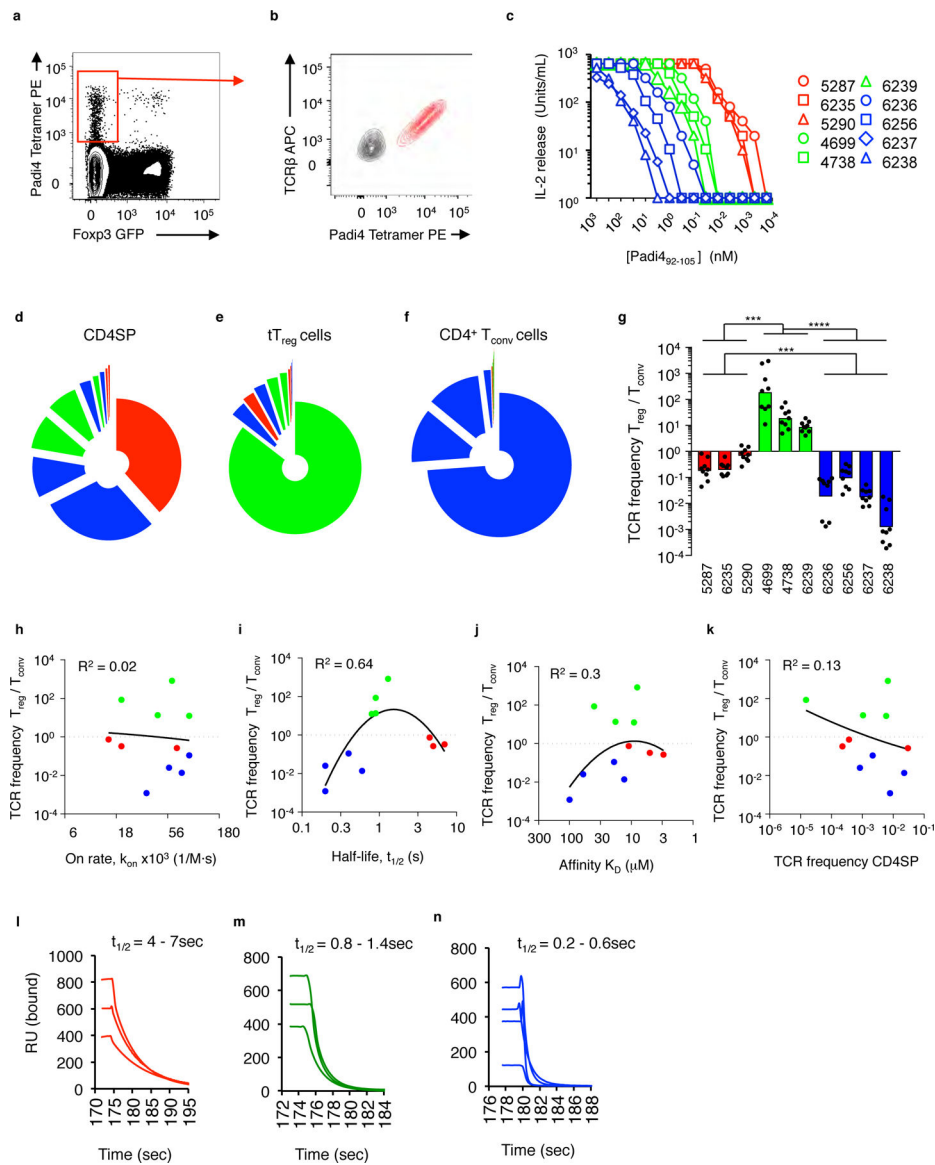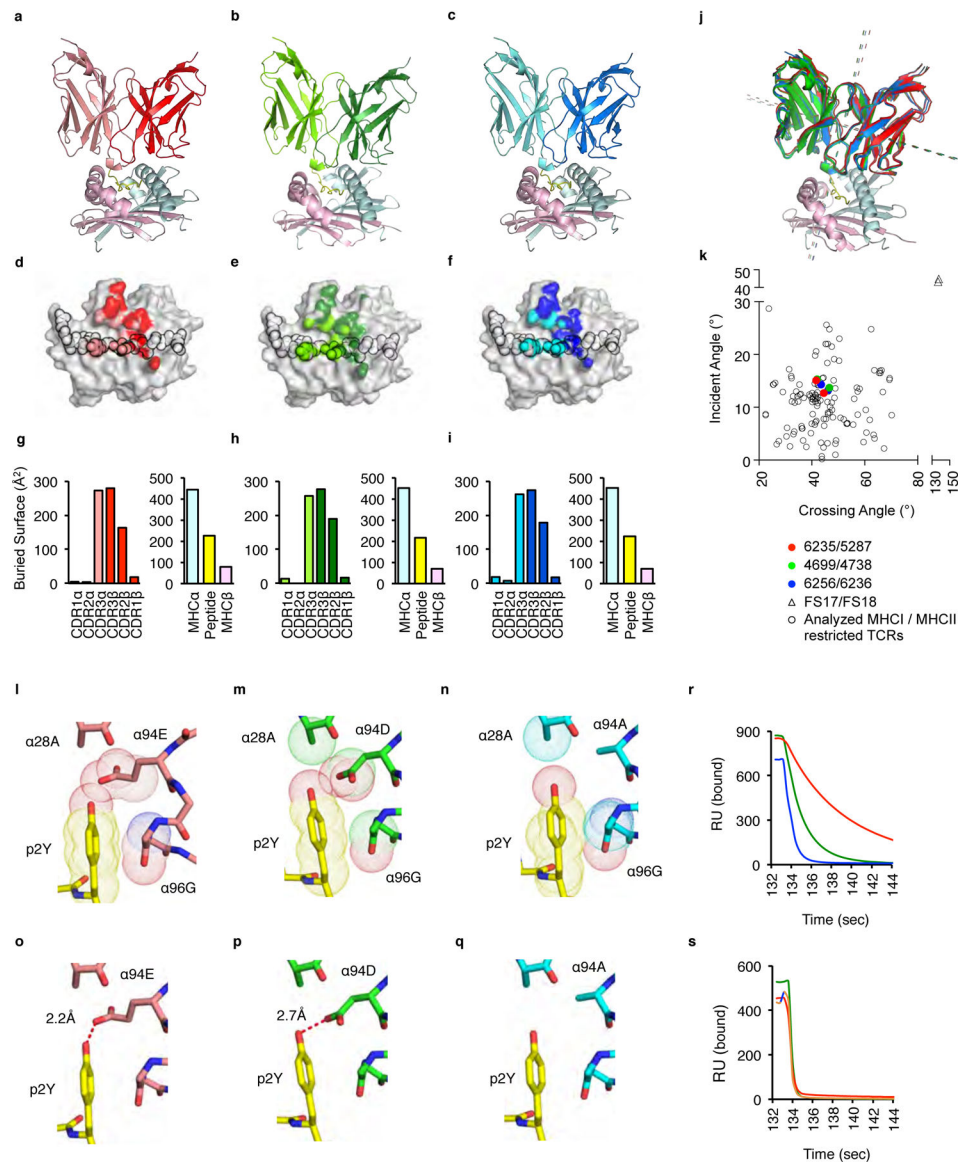
Figure 7.

Padi4-specific neonatal tT_{reg} cells express TCRs with modest dwell times. (**a**) IA^b-Padi4 tetramer^{pos} $V\alpha2^+$ Foxp3-GFP^{neg} CD4SP thymocytes isolated from YAe62β.*Foxp3-GFP* were sorted, and (**b**) TCRs cloned and re-expressed in T cell hybridomas. (**c**) IL-2 response of Padi4-reactive T cell hybridomas cultured with IA^b-expressing fibroblasts and titrating concentration of soluble Padi4$_{92-105}$ peptide; see key for name of individual TCRs. (**d-f**) Relative distribution of Padi4-reactive TCR clonotypes carried in the (**d**) thymic Foxp3-GFP^{neg} CD4SP, (**e**) splenic CD4$^+$ Foxp3-GFP^{pos} tT_{reg} and (**f**) splenic CD4$^+$ Foxp3-GFP^{neg} T_{conv} cell repertoires of 2-week old YAe62β.*Foxp3-GFP* mice. Colored pie slices represent individual TCRs described in (**c**). (**g**) Frequency distribution of individual Padi4-reactive T cell clonotypes carried in splenic CD4$^+$ tT_{reg} versus CD4$^+$ T_{conv} cell repertoires of 2-week old YAe62β.*Foxp3-GFP* mice. Data are derived from 4 independent experiments, (d-f) represented as mean fraction of repertoire, (g) bars represent the data geometric mean. (**h-k**)

Centered second order non-linear regression analysis of 11 Padi4- and Add2-specific TCRs comparing the tT_{reg}/T_{conv} cell frequency bias versus the TCR:self-pMHC (**h**) on-rate, k_{on} (**i**) half-life, $t_{1/2}$ and (**j**) equilibrium affinity, K_D, and (**k**) the clonal frequency in Foxp3^{neg} CD4SP thymocytes. Correlation plots are based on probable cure fit using Akaike's Information Criteria, Prism 7.04. R^2 values represent goodness of fit analysis. (**l-n**) Time scale of soluble (**l**) 5287, 6235, 5290, (**m**) 4699, 4783, 6239, and (**n**) 6236, 6256, 6237, 6238 TCRs disassociating from immobilized IA^b-Padi4 measured by surface plasmon resonance. Sensograms are background subtracted from each TCR interacting with a non-cognate ligand. Data are derived from 4 biological replicates with similar results. (g) Significance identified using a Kruskal-Wallis test and Dunn's multiple comparisons test, ***P<0.001, ****P<0.0001.

Figure 8.

TCRs that promote neonatal negative selection, tT$_{reg}$ differentiation or CD4 T$_{conv}$ cell development use conventional docking orientations on IA^b-Padi4. (**a-c**) Ribbon diagrams of (**a**) 6235 (pdb: 6MNO), (**b**) 4699 (pdb:6MKD) and (**c**) 6256 (pdb: 6MNM) TCRs binding IA^b-Padi4. The 6235 TCR is colored red (TCRβ) and pink (TCRα); the 4699 TCR is colored dark green (TCRβ) and light green (TCRα); The 6256 TCR is colored dark blue (TCRβ) and light blue (TCRα). IA^b-Padi4 is colored cyan (IA^{b}α chain), yellow (peptide), and magenta (IA^{b}β chain). (**d-f**) Projections of the (**d**) 6235, (**e**) 4699 and (**f**) 6256 TCRs bound to IA^b-Padi4. The peptide residues are outlined in black. (**g-i**) The amount of buried surface area (BSA) of the (**g**) 6235:IA^b-Padi4, (**h**) 4699:IA^b-Padi4 and (**i**) 6256:IA^b-Padi4 complexes contributed by TCRα and TCRβ loops, and the peptide or MHC chains. Figures were made with PyMol. (**j**) Overlay of 6235, 5287, 4699, 4378, 6256 and 6236 TCRs binding IA^b-Padi4. Dashed lines indicate the crossing and incident angles. (**k**) Plot of the

6235, 5287, 4699, 4378, 6256 and 6236 TCR:IA^b-Padi4 crossing and incident angles, compared to 129 human and mouse MHC-I and MHC-II TCR:pMHC complexes, including two iT$_{reg}$ reverse orientation (triangles)[44]. (**l-q**) Van der Waals interactions between the (**l**) 6235, (**m**) 4699 and (**n**) 6256 TCRα chains with the Padi4 P2Y residue, and (**o-q**) the presence, absence and distance of a hydrogen bond (red dash line) between the CDR3α 94 residue and the Padi4 P2Y hydroxyl moiety. (**r**, **s**) Time scale of soluble 6235 (red), 4699 (green) and 6256 (blue) TCRs disassociating from immobilized (**r**) IA^b-Padi4 and (**s**) IA^b-Padi4 p2F measured by surface plasmon resonance. Sensograms are background subtracted from each TCR interacting with a non-cognate IA^b-Add2 ligand. SPR data are examples of 4 independent experiments, giving similar results.